


Cite this: *RSC Adv.*, 2024, 14, 27504

# Detecting dissolved mercury(II) ions using chitosan-AgNP strips integrated with smartphones

Muhammad Adlim,<sup>a</sup> Muhammad Syukri Surbakti,<sup>c</sup> Ahmad Fairuz Omar,<sup>d</sup> Ratu Fazlia Inda Rahmayani,<sup>b</sup> Abdul Haris Hasmar,<sup>e</sup> Ismail Ozmen,<sup>f</sup> and Musa Yavuz<sup>g</sup>

A simple preparation of a paper strip test with a smartphone-based instrument for detecting dissolved mercury is still in development. This study aims to develop a smartphone-based colorimetric paper strip test using chitosan-stabilized silver nanoparticles for detecting dissolved mercury. The method demonstrated high sensitivity and selectivity for  $Hg^{2+}$  ions, with detection limits comparable to UV-vis spectrophotometry. Silver ions embedded in the chitosan matrix were reduced by either sodium  $NaBH_4$  or  $N_2H_4$ . Both chi-AgNP colloidal and chi-AgNP paper strips were tested for sensitivity of mercury(II) solution detection with and without ion interference. The accuracy of colour change responding to the mercury concentration was recorded with several smartphones in a handmade cubical and a T-shape micro-studio. Only  $NaBH_4$  gives colloidal chi-AgNPs relatively dispersed, and the colloidal chi-AgNPs become aggregated when AgNP interacts with mercury(II) ions. The colour change of chi-AgNP paper strips responding to the concentration of mercury(II) and quantified using a smartphone is consistent when confirmed with UV-vis spectrophotometric determination with a comparable limit of detection ( $0.76 \mu M$ ). The inferring ions do not significantly affect mercury(II) analyses. Therefore, the paper strip integrated with the smartphone is effectively used for mercury(II) detection in water as long as the mercury concentration is  $>1 \mu M$ . This finding might inspire advanced technology with a larger number of data references, and machine learning involvement to develop more compatible and simple mercury detection.

Received 7th July 2024  
Accepted 24th August 2024

DOI: 10.1039/d4ra04901b

rsc.li/rsc-advances

## 1. Introduction

Silver nanoparticles (AgNPs) have been widely used to monitor heavy metal ion pollution, including dissolved mercury. Due to their wide surface-to-volume ratio and the presence of surface plasma resonance (SPR) bands, AgNPs have high sensitivity and good selectivity. SPR is a characteristic of metal nanoparticles that provides a distinctive colour in the visible light spectrum.

Mercury(II) ions are water-soluble, thereby easily polluting the food chain.<sup>1</sup> Mercury(II) can be detected with various instruments

such as an Atomic Absorption Spectrometer (AAS), Inductive Coupled Plasma-Mass Spectrometer (ICP-MS), and Atomic Fluorescence Spectrometer (AFS), however, they are expensive, require specialized skills, and are not portable.<sup>2</sup> Alternative methods, such as colorimetric tests based on color changes, are being developed, but many are still used for qualitative measurement.

Several AgNP-based colorimetric paper-strip tests for detecting mercury(II) ions have been reviewed and published.<sup>3–6</sup> They have been used as several protection agents but the use of chitosan is still being developed.<sup>7</sup> Studies integrating a chitosan-based paper strip test with a handphone are still rare<sup>8–11</sup> and most studies focused on AgNP preparation with a complex procedure.<sup>12</sup> A large number of papers on the green synthesis of silver nanoparticles have already been published including papers on green tea extract and other plant extracts used in silver nanoparticle preparation, some either as the reducing agent only or as both the reducing agent and the stabilizer for silver.<sup>13–17</sup> However, the plant extract and the life cells are easily decomposed; then, special handling is required in long-term application. This study aims to develop a cost-effective, easy-to-use, and portable method for mercury detection using chitosan-stabilized silver nanoparticles and smartphone integration. This study used chitosan as a stabilizer for silver used

<sup>a</sup>Graduate School of Mathematics and Applied Science, Universitas Syiah Kuala, Darussalam, Banda Aceh, 23111, Indonesia. E-mail: adlim@usk.ac.id

<sup>b</sup>Chemistry Department, FKIP, Universitas Syiah Kuala, Darussalam, Banda Aceh, 23111, Indonesia

<sup>c</sup>Physics Department, FMIPA, Universitas Syiah Kuala, Darussalam, Banda Aceh, 23111, Indonesia

<sup>d</sup>School of Physics, Universiti Sains Malaysia, Minden, Pulau Pinang 11800, Malaysia

<sup>e</sup>Islamic Education Department, FTK UIN Ar-Raniry Banda Aceh, Darussalam, Banda Aceh, 23111, Indonesia

<sup>f</sup>Department of Chemistry, Faculty of Engineering and Nature Sciences, Suleyman Demirel University, Isparta, 32260, Turkey

<sup>g</sup>Animal Science Department, Agriculture Faculty, Isparta University of Applied Sciences, Isparta, 32260, Turkey



in paper strip preparation, which is well known, especially when integrated with smartphones.<sup>18,19</sup> The objectives of this study are to (1) develop a chitosan-stabilized silver nanoparticle-based paper strip for detecting mercury(II) ions, (2) integrate the detection method with smartphones for on-site quantification, and (3) evaluate the sensitivity, selectivity, and practical applicability of the developed method.

## 2. Methods

### 2.1 Materials, instruments, and tools

The materials used include chitosan (medium molecular weight), AgNO<sub>3</sub>, N<sub>2</sub>H<sub>4</sub>, NaBH<sub>4</sub>, mercury(II) nitrate, lead(II) nitrate, cadmium(II) nitrate, zinc(II) nitrate, calcium(II) nitrate, copper(II) nitrate, manganese(II) nitrate, aluminum(III) nitrate, potassium nitrate, sodium nitrate, cobalt(II) nitrate, nickel(II) nitrate, magnesium(II) nitrate and iron(II) sulfate. All of these nitrate salts were purchased from Merck with PA grades without further purification. The water samples used were river water, well water, PDAM water, and plastic bottled drinking water. The instruments used were a UV-vis spectrophotometer Shimadzu 1800, TEM Jeol JEM-1400 operating at 100 kV, smartphone ASUS ZenFone 3 Max (ZC533KL) Android version 8.1.0 with 16 MP camera, smartphone Samsung Galaxy J5 Prime (SM-G570Y/DS), android version 7.1.2 with 13 MP camera, Xiaomi Redmi 5 Plus smartphone, android version: 7.1.2 with 12 MP camera. Handmade assembled equipment to integrate handphone and sample probe namely cuboid-controlled-light and T-shape-controlled-light instrument.

### 2.2 Preparation and characterization of chi-AgNPs as the active material for chi-AgNP paper strips

The preparation of colloidal silver nanoparticles in a chitosan matrix using either NaBH<sub>4</sub> (Nb) or N<sub>2</sub>H<sub>4</sub> (Hz) as the reducing agents was verified according to the previous methods.<sup>20,21</sup> Chitosan stock solution was made by dissolving 6 mg of chitosan per ml of 1.5% aqueous acetic acid solution (AAAS). Chitosan stock solution ( $5.6 \times 10^{-4}$  monomer mole) was diluted with 88.8 ml of aqueous acetic acid (1.5%) and 90 ml of methanol. While stirring, silver ion stock solution ( $1.12 \text{ ml}$  or  $1.12 \times 10^{-4}$  mole) was added drop wisely into the chitosan solution. NaBH<sub>4</sub> (5 times more than the silver ion moles) was added. The completeness of reduction was followed based on color changes monitored with a spectrophotometer. The experiment was repeated by substituting NaBH<sub>4</sub> with N<sub>2</sub>H<sub>4</sub>. The particle size of chi-AgNP(Nb) and chi-AgNP(Hz) before and after mixing with mercury(II) ions was characterized by TEM.

After studying the colloidal chitosan silver nanoparticles and screening the best preparation method to give smaller and dispersed silver particles, the colloidal silver nanoparticles possessing dispersed and small-sized particles were immobilized on the filter papers (1 cm × 1 cm) by dipping method.

### 2.3 Selectivity test of chi-AgNP paper strip toward mercury(II) ions among other metal ions

The selectivity of the chi-AgNP towards mercury(II) ions was evaluated by dipping the paper strip in various metal ions and

comparing its response to mercury(II). The metal ions tested including Al<sup>3+</sup>, Ba<sup>2+</sup>, Ca<sup>2+</sup>, Cd<sup>2+</sup>, Cr<sup>3+</sup>, Co<sup>2+</sup>, Cu<sup>2+</sup>, Fe<sup>2+</sup>, K<sup>+</sup>, Mg<sup>2+</sup>, Mn<sup>2+</sup>, Na<sup>+</sup>, Ni<sup>2+</sup>, Pb<sup>2+</sup>, and Zn<sup>2+</sup> at a concentration of 10 μM. The response was observed after 10 minutes of mixing with chi-AgNP(Nb) or chi-AgNP(Hz).

### 2.4 Interfering ion test in determination of mercury(II) ions using chi-AgNP paper strips

Paper strips ready for use are also tested for their response to interfering ions. Mercury(II) ions was mixed with several diluted metal ions that are common in water: Cr<sup>3+</sup>, Mn<sup>2+</sup>, Fe<sup>2+</sup>, Mn<sup>2+</sup>, Co<sup>2+</sup>, Ni<sup>2+</sup>, Cd<sup>2+</sup>, Cu<sup>2+</sup>, Zn<sup>2+</sup>, Al<sup>3+</sup>, Pb<sup>2+</sup>, Mg<sup>2+</sup>, Ca<sup>2+</sup>, Ba<sup>2+</sup>, Na<sup>+</sup>, and K<sup>+</sup>. The paper strip responses to mercury(II) ions were compared with and without ion interference.

### 2.5 Sensitivity test of chi-AgNP paper strips on the determination of mercury(II) ions

A total of 4 ml of mercury(II) ion solution with various concentrations (0.2 μM to 10 μM) was mixed with 0.2 μL chi-AgNP(Nb) colloidal solution. This mixture was stirred and incubated for 5–10 minutes at room temperature, and then the UV-vis spectra were measured. Sample simulation was prepared by dissolving Hg(NO<sub>3</sub>)<sub>2</sub>·H<sub>2</sub>O crystals in conc. HNO<sub>3</sub>. After the crystals dissolved, the conc. HNO<sub>3</sub> excess was evaporated in a water bath before diluting with distillate water. The stock solution was diluted in various concentrations and used as simulated samples. Using similar samples and treatment, the mercury content was determined by using the paper strip. Colourimetric colour changes of the paper strip before and after adding mercury(II) ions were also measured in micro studio (T-shape and cuboid-controlled light) instruments. The micro studio is integrated with a smartphone from 3 brands: Asus®, Samsung®, and Xiaomi®.

### 2.6 Quantification of colour change using a smartphone with cuboid-controlled light and T-shape instruments as the micro-studio

The experiment was repeated the colour changes were recorded using a smartphone in two types of micro studios (cuboid and T-shape). The mean of red, green, and blue (RGB) data was plotted with [Hg<sup>2+</sup>] standard (simulation samples) and then calibrated with UV-vis.

### 2.7 Detection limit of chi-AgNP(Nb) integrated smartphone for mercury(II) ions

The sensitivity test of the paper strip integrated with a smartphone was a similar method with colloidal chi-AgNP(Nb). However, the colloidal solution was substituted with a paper strip, and the colour change was recorded with a smartphone in the micro studio. The finding was compared with UV-vis measurement data.

### 2.8 Analysis of mercury(II) ions within the actual water sample by using chi-AgNP paper strips

The procedure of Section 2.4 was repeated by determining the dissolved mercury using a UV-vis spectrophotometer and



a paper strip. These methods were applied for the determination of mercury content within river water samples, sink water, well water, and commercial mineral water. Samples were taken around the Syiah Kuala University campus. Before analysis, water samples were acidified with HCl around pH  $\sim$ 1 and kept in sealed plastic bottles at room temperature.

### 2.9 Expiry period of chi-AgNP(Nb)

Several paper strips were kept in paper bags to control the moisturize. Every week, the color change of the paper strip was monitored, taken the picture, recorded, and compared with fresh paper strip photographs. The sensitivity was re-tested on mercury determination.

## 3. Results and discussion

The research findings and discussion are focused on elaborating the characteristics of colloidal and paper strip chi-AgNPs. The efficacy of dissolved mercury detection integrated with a mini-studio equipped with a smartphone is represented by the selectivity (only on mercury(II) ions) and the sensitivity (limit of detection) of the paper strip toward mercury(II) ions in simulated samples. Testing on the presence of other ions during

mercury detection is also discussed. Finally, the paper strip was applied to actual water samples. The findings were compared with UV-vis spectrophotometric analysis.

### 3.1 Characterization chi-AgNPs as the active material for chi-AgNP paper strips

Characterization of chi-AgNPs is represented by the particle size and the particle distribution. Small size and dispersed particles with narrow size distribution are preferable in nanomaterial theory since they usually have high surface area and induce better reactivity.

The TEM image of chi-AgNP(Hz) shows much more aggregation than chi-AgNP(Nb), as presented in Fig. (1a) and (c). Hydrazine is reactive as a reducing agent for silver ions and also causes a change in the surface chemistry of AgNPs, including weakening the stabilizer function. Consequently, more significant aggregation occurs.<sup>22</sup> Both these colloidal silver nanoparticles sensitively responded to the mercury ions by growing bigger and more aggregated particles (Fig. (1b) and (d)). The AgNPs become closer after adding mercury ions (as the analyte), triggering agglomeration, as an analogy to the previous report.<sup>23</sup> Mercury(II) ions links AgNPs with each other due to a chemical reaction between AgNP and mercury(II) ions. Interaction between AgNPs with mercury(II)

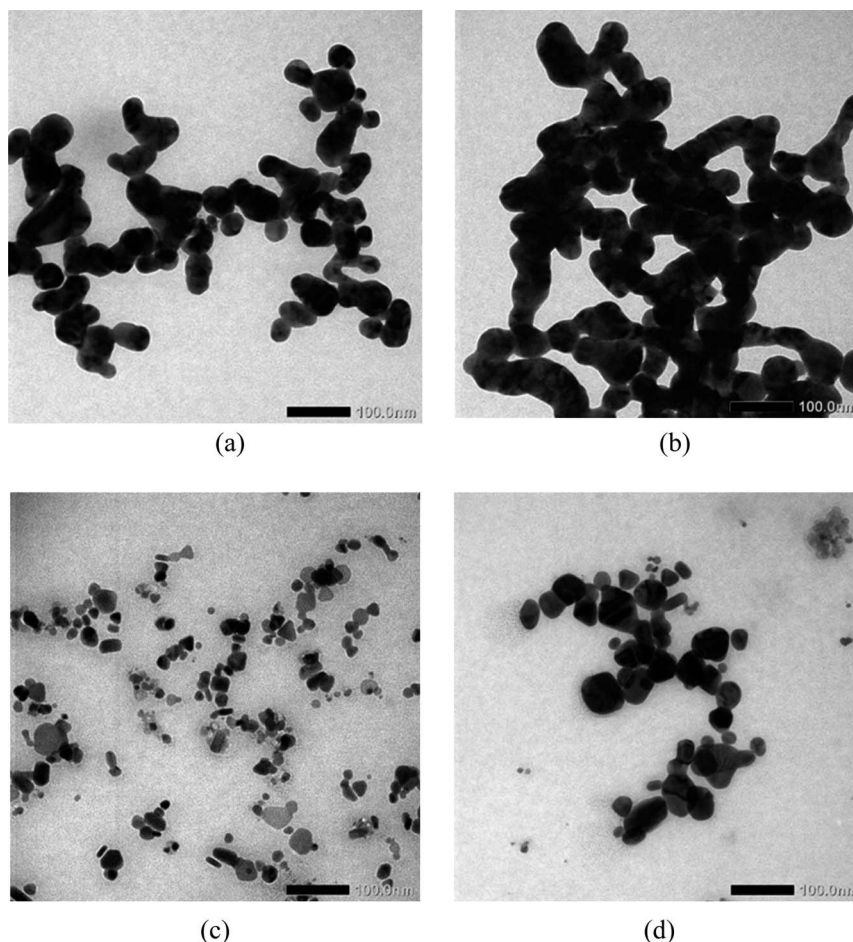


**Fig. 1** (a) TEM of chi-AgNP(Hz) without the addition of mercury(II) ions. (b) TEM of chi-AgNP(Hz) after the addition of mercury(II) ions. (c) TEM of chi-AgNP(Nb) without the addition of mercury(II) ions. (d) TEM of chi-AgNP(Nb) after addition of mercury(II) ions.



ions involve several mechanisms. AgNPs Adsorbed mercury(II) ions on the surface of AgNPs, which subsequently follows with a reduction of  $\text{Hg}^{2+}$  to  $\text{Hg}^0$  due to the reduction potential of  $E^\circ(\text{Hg}^{2+}/\text{Hg}) < E^\circ(\text{Ag}^+/\text{Ag})$ . Since mercury(II) ions are just a trace amount, thereby, not all AgNPs are oxidized by mercury(II) into silver ions; some remain as silver metal, and then both metals form an amalgam of (Hg/Ag). Oxidizing partially AgNPs, which are brown, into  $\text{Ag}^+$  ions that are colorless is a phenomenon of color change during mercury analysis.

### 3.2 Selectivity of chi-AgNP paper strip toward mercury(II)

In actual samples, mercury is mixed with other ions; therefore, the selectivity of the paper strip to the mercury ion only is crucial; otherwise, the determination becomes vague.

Since chi-AgNP(Hz) has a dark colour and highly aggregated particles, which might cause difficulty in UV-vis spectrophotometric analysis, then it was excluded from further experimental

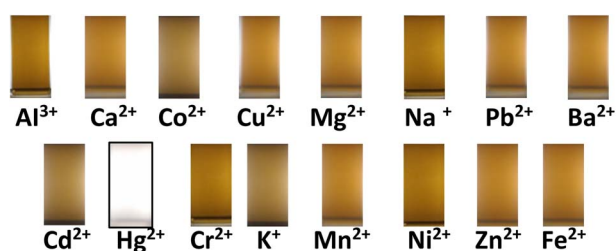


Fig. 2 Colour changes of chi-AgNP(Nb) in the presence of various metal ions.

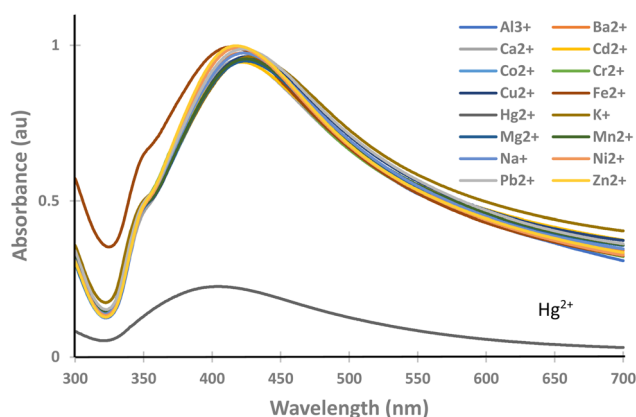


Fig. 3 UV-vis spectra of chi-AgNP(Nb) in the presence of various metal ions.

works and focused on chi-AgNP(Nb) only. The chi-AgNP(Nb) paper strip selectivity towards mercury(II) ions is different from other ions ( $\text{Al}^{3+}$ ,  $\text{Ba}^{2+}$ ,  $\text{Ca}^{2+}$ ,  $\text{Cd}^{2+}$ ,  $\text{Cr}^{3+}$ ,  $\text{Co}^{2+}$ ,  $\text{Cu}^{2+}$ ,  $\text{Fe}^{2+}$ ,  $\text{K}^+$ ,  $\text{Mg}^{2+}$ ,  $\text{Mn}^{2+}$ ,  $\text{Na}^+$ ,  $\text{Ni}^{2+}$ ,  $\text{Pb}^{2+}$ , and  $\text{Zn}^{2+}$ ) at a concentration of  $10 \mu\text{M}$  after 10 minutes of mixing with chi-AgNP(Nb). As shown in Fig. 2, only the sample solution containing mercury(II) ions shows a significant colour change from brown to colourless, while the other ions remain brown. The colour change with mercury(II) ions can be easily observed. This is also confirmed by the UV-vis spectra shown in Fig. 3. This means that chi-AgNP(Nb) is highly selective towards mercury(II) ions compared to other ions.

The selectivity phenomenon might be explained based on the thermodynamic feasibility of the redox reaction. The Silver metal nanoparticle has a dark brown, and has reduction potential,  $E^\circ_{\text{red}}(\text{Ag}^+/\text{Ag}^0)$  of +0.7996 Volt which is larger than  $E^\circ_{\text{red}}(\text{M}^{n+}/\text{M}^0)$  of other ions listed in Fig. 2, except  $E^\circ_{\text{red}}(\text{Hg}^{2+}/\text{Hg}^0)$ , which has +0.854, larger than  $E^\circ_{\text{red}}(\text{Ag}^+/\text{Ag}^0)$ . Therefore, the redox reaction between the ions with silver nanoparticles is not thermodynamically feasible since silver cannot lower the oxidation state, and other ions are not thermodynamically feasible to oxidize further by silver nanoparticles, due to the  $\Delta E^\circ$  (negative); then  $\Delta G^\circ$  becomes positive.

The interaction of silver nanoparticles with mercury(II) ions causes a redox reaction since the  $\Delta E^\circ$  is positive or thermodynamically feasible.  $E^\circ_{\text{red}}(\text{Hg}^{2+}/\text{Hg}^0) > E^\circ_{\text{red}}(\text{Ag}^+/\text{Ag}^0)$ , silver metal reduced the mercury(II) ion, and silver metal is oxidized into silver ions (colourless) as indicated by colour change of the paper strip from brown to colourless.

### 3.3 Interfering ion test

Since mercury is possibly mixed with other ions, the effect of other ions might interfere with mercury detection. The detection becomes less obvious, less reliable, etc. The paper strip of chi-AgNP(Nb) detects mercury(II) ions by changing its colour from brown to colourless although the sample containing several other dissolved metal ions ( $\text{Cr}^{3+}$ ,  $\text{Mn}^{2+}$ ,  $\text{Fe}^{2+}$ ,  $\text{Mn}^{2+}$ ,  $\text{Co}^{2+}$ ,  $\text{Ni}^{2+}$ ,  $\text{Cd}^{2+}$ ,  $\text{Cu}^{2+}$ ,  $\text{Zn}^{2+}$ ,  $\text{Al}^{3+}$ ,  $\text{Pb}^{2+}$ ,  $\text{Mg}^{2+}$ ,  $\text{Ca}^{2+}$ ,  $\text{Ba}^{2+}$ ,  $\text{Na}^+$ , and  $\text{K}^+$ ). This means mercury detection is free from interfering with other ions. The paper strip effectively detects mercury(II) ions with and without other ion presence, as shown in Fig. 4.

### 3.4 Testing the sensitivity of the chi-AgNP(Nb) paper strip to various mercury(II) ion concentrations

The sensitivity of paper strips in a diluted solution of mercury is significant to differentiate the colour change, especially in direct observation (only visual look without an instrument).

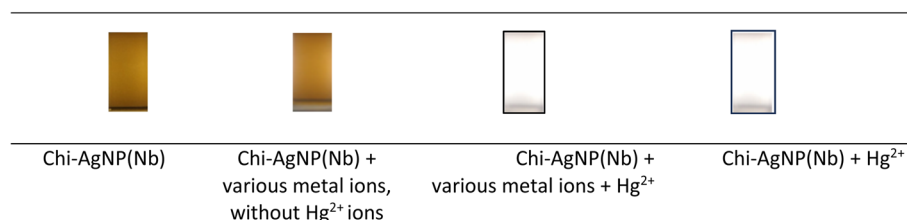


Fig. 4 Colour changes of chi-AgNP(Nb) in solutions containing various ions.



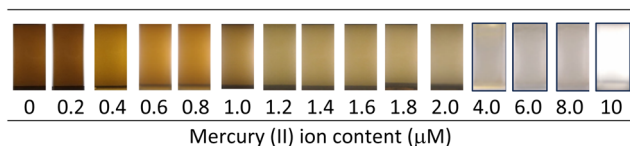


Fig. 5 Colour changes of chi-AgNP(Nb) paper strips responding to various mercury(II) ion concentrations.

The colour change of chi-AgNP(Nb) from brown to gradually fading and finally colourless, along with an increase in mercury(II) concentration (Fig. 5). The paper strip sensitivity as shown by obvious colour changes was as low as 0.4  $\mu\text{M}$ . This is also consistent with UV-vis spectra at 400 nm of colloidal chi-AgNP(Nb) when it reacts to various mercury concentrations, as presented in Fig. 6.

It was predicted that the chi-AgNP(Nb) plasmon band would shift to a longer wavelength due to the particle aggregation when it interacted with mercury ions, as deduced from TEM images (Fig. 1). However, as shown in Fig. 6 the spectra shifted to a shorter wavelength and shaper shape, which are inverse spectra characteristic of the common colloidal silver plasmon (without other metal presence) that usually shifts to a higher wavelength when the colloidal silver particle size increases.<sup>24</sup> These phenomena confirmed the chi-AgNP(Nb) sensitivity toward mercury ions.

The colour changes of chi-AgNP(Nb) paper strips responding to various mercury(II) ion concentrations correlate to the chemical reaction completeness of silver metal nanoparticles and mercury(II) ions.  $\text{Ag}^0$  (brown) is completely oxidized into  $\text{Ag}^+$  (colourless) by a sufficient amount (high concentration) of mercury(II) ions then, it turns into a fully colourless paper strip as shown Fig. 5. However at a lower concentration of mercury(II) ions, the silver metal nanoparticle just became fade colour due to the partial oxidation, and consequently, the remain  $\text{Ag}^0$  still gave the brownish colour.

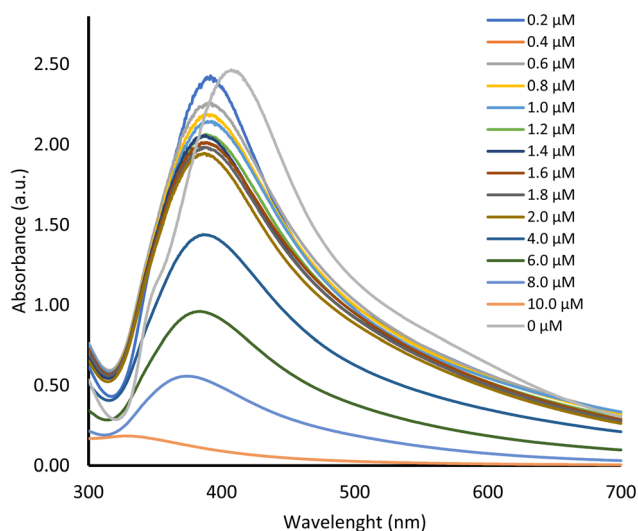


Fig. 6 UV-vis spectra of chi-AgNP(Nb) with the addition of various mercury(II) ion concentrations.

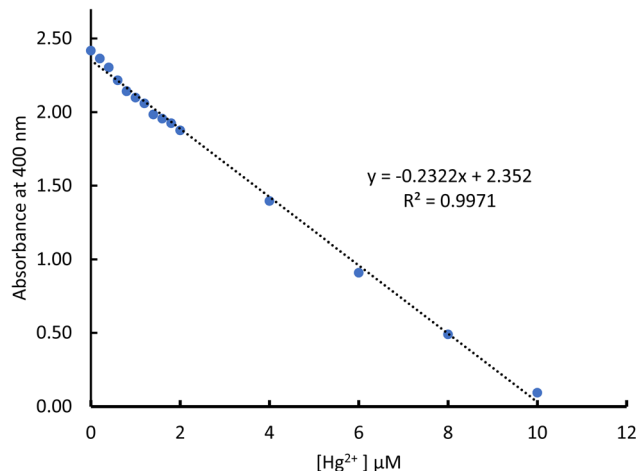


Fig. 7 Plot of linearity of differences in absorbance intensity at a wavelength of 400 nm against various mercury(II) ion concentrations.

The absorbance decreased consistently along with an increase in mercury(II) ions as presented in Fig. 6. Data from Fig. 6 are plotted between the absorbance change and concentration of mercury(II) ion detection and gave a consistent correlation with linear regression equation of  $y = -0.2322x + 2.352$ , with the coefficient determination of  $R^2 = 0.99$  (Fig. 7). These data confirmed the colour change in the chi-AgNP(Nb) paper strip responding to the mercury(II) ion detection within the samples.

### 3.5 Quantification of color change using a smartphone with cuboid-controlled light and T-shape instruments as the micro-studio

Numerical quantification of chi-AgNP(Nb) colour change representing the mercury concentration is deduced from RGB measurement by using a smartphone. Micro-studios were developed to give uniform conditions for photographing the chi-AgNP(Nb) paper-strip colour change. These micro-studios were named cuboid controlled-light (Fig. 8b) and T-shape instruments as illustrated in Fig. 8b. These microstudios were assembled with alkaline batteries and LED light, an on-off switch, reflective surface/mirror, sample/object holder, cellular phone support, and a photographing hole that makes the photographed image directly sent to the laptop. These microstudios were customized handmade assembled, not commercially available, and for the first time published here.

The sensitivity test of the chi-AgNP(Nb) paper strip test toward various mercury(II) ions concentrations apart from UV-vis, was measured simultaneously using 2 types of micro-studio and 3 brands of smartphone. The RGB data analyzed using the Color Grap Apps® representing the mercury concentration are tabulated in Table 1. The mean of R, G, and B for each data set in Table 1 represents the RGB coordinate plotted against the mercury(II) concentration.

The linearity plot of the average RGB value against various mercury(II) ion concentrations using two instruments with 3 types of smartphones is shown in Fig. 9. By plotting RGB data against mercury concentration, it can be suggested that no matter which





Fig. 8 Micro-studios for controlling light; (a) cuboid and (b) T-shape models.

Table 1 RGB data for mercury(II) ion testing with chi-AgNP(Nb)

| Hg <sup>2+</sup> (μM) | Cuboid controlled-light instrument |     |     |         |     |     |        |     |     | T-shape controlled-light instrument |     |     |         |     |     |        |     |     |
|-----------------------|------------------------------------|-----|-----|---------|-----|-----|--------|-----|-----|-------------------------------------|-----|-----|---------|-----|-----|--------|-----|-----|
|                       | Asus                               |     |     | Samsung |     |     | Xiaomi |     |     | Asus                                |     |     | Samsung |     |     | Xiaomi |     |     |
|                       | R                                  | G   | B   | R       | G   | B   | R      | G   | B   | R                                   | G   | B   | R       | G   | B   | R      | G   | B   |
| 0                     | 212                                | 153 | 78  | 152     | 125 | 65  | 219    | 169 | 65  | 132                                 | 103 | 90  | 77      | 58  | 53  | 117    | 88  | 83  |
| 0.2                   | 190                                | 168 | 93  | 151     | 130 | 71  | 201    | 171 | 88  | 134                                 | 105 | 92  | 69      | 67  | 61  | 121    | 92  | 86  |
| 0.4                   | 193                                | 169 | 96  | 156     | 134 | 73  | 202    | 174 | 91  | 152                                 | 118 | 73  | 80      | 70  | 57  | 133    | 97  | 78  |
| 0.6                   | 196                                | 173 | 98  | 159     | 137 | 75  | 202    | 175 | 101 | 154                                 | 121 | 77  | 84      | 74  | 61  | 130    | 101 | 89  |
| 0.8                   | 204                                | 173 | 101 | 162     | 141 | 76  | 207    | 181 | 103 | 161                                 | 123 | 75  | 91      | 79  | 62  | 139    | 107 | 89  |
| 1.0                   | 206                                | 174 | 104 | 165     | 145 | 79  | 212    | 184 | 105 | 155                                 | 125 | 93  | 93      | 83  | 64  | 140    | 108 | 96  |
| 1.2                   | 207                                | 177 | 109 | 169     | 147 | 81  | 228    | 185 | 96  | 157                                 | 127 | 95  | 96      | 86  | 68  | 140    | 113 | 102 |
| 1.4                   | 208                                | 178 | 112 | 169     | 148 | 87  | 216    | 189 | 113 | 160                                 | 133 | 93  | 101     | 89  | 70  | 146    | 118 | 105 |
| 1.6                   | 209                                | 180 | 116 | 172     | 151 | 88  | 214    | 191 | 117 | 157                                 | 143 | 101 | 114     | 93  | 64  | 151    | 122 | 107 |
| 1.8                   | 200                                | 185 | 130 | 174     | 153 | 89  | 210    | 190 | 128 | 169                                 | 141 | 101 | 112     | 97  | 72  | 155    | 124 | 109 |
| 2.0                   | 214                                | 184 | 121 | 180     | 152 | 91  | 215    | 194 | 130 | 164                                 | 148 | 108 | 114     | 100 | 73  | 161    | 129 | 107 |
| 4.0                   | 229                                | 201 | 153 | 183     | 175 | 127 | 226    | 211 | 160 | 206                                 | 176 | 127 | 145     | 132 | 99  | 191    | 160 | 126 |
| 6.0                   | 241                                | 219 | 184 | 205     | 193 | 154 | 239    | 229 | 192 | 224                                 | 200 | 170 | 166     | 160 | 135 | 205    | 185 | 167 |
| 8.0                   | 254                                | 239 | 216 | 216     | 211 | 193 | 252    | 243 | 214 | 241                                 | 225 | 215 | 191     | 189 | 172 | 220    | 211 | 209 |
| 10                    | 255                                | 255 | 254 | 226     | 230 | 227 | 255    | 253 | 255 | 255                                 | 254 | 241 | 211     | 214 | 213 | 228    | 233 | 247 |

micro-studio and smartphone are used, the linear response of chi-AgNP(Nb) toward mercury concentration enhancement is consistent; therefore, using chi-AgNP(Nb) as a paper strip for detecting dissolved mercury(II) ions recorded with a smartphone equipped with micro-studio is reasonably used as a quantitative analysis.

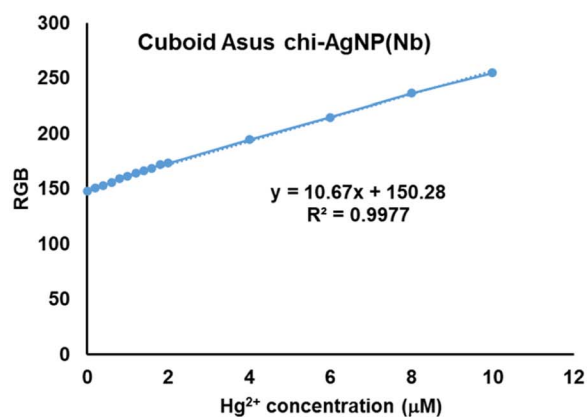
### 3.6 Detection limit of chi-AgNP(Nb) integrated smartphone for mercury(II) ions

The detection limit (LoD), which is the lowest analyte concentration that can be detected, and the quantification limit (LoQ), which is the lowest analyte concentration that can be detected quantitatively, are determined based on the formulas  $\text{LoD} = 3.3 \times \text{SD intercept/slope}$  and  $\text{LoQ} = 10 \times \text{SD intercept/slope}$ , respectively<sup>25,26</sup> (Vashist & Loung, 2018a). The intercept and slope are obtained from the linearity plot of absorbance or average RGB against various concentration variations (Fig. 9). The LoD and LoQ calculations are summarized in Table 2.

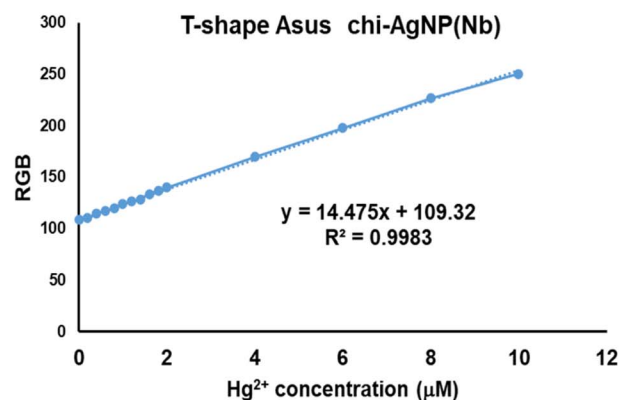
Table 2 shows that in cuboid instruments; Asus and Samsung smartphones are more sensitive to detecting mercury ions than Xiaomi cellular phones, as indicated by the smaller LoD and LoQ.

These trends are consistent when using a T-shape instrument, but using a T-shape gave better detection than using the cuboid. Overall, the detection capacity is comparable to UV-vis LoD and LoQ, except for using a Xiaomi cellular phone, which lowers detection sensitivity. However, according to the *F* test, those series are not significantly different from the UV-vis method (at  $0.05\alpha$ ). Several factors can cause the sensitivity variance of the cellular phone, mainly the camera specification, the image resolution, the pixel size, and the detection of a smartphone-based analyte.<sup>9</sup> By using a smartphone photo camera as a 'smart detector', complementary metal oxide semiconductor (CMOS) image sensors functioning as a 'smart recorder', an application that acts as a 'smart readout', almost all optical-based detection methods can be integrated.<sup>27</sup>

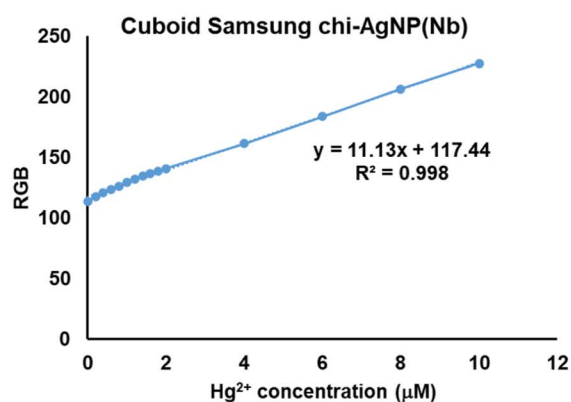
Smartphones for image capture and image processing using Android applications such as Color Grap combined with cuboid and T-shape instruments not only save time but also provide good results for the detection of mercury(II) ions using chi-AgNP(Nb). In addition, this instrument provides digital data and portability for on-the-spot detection.



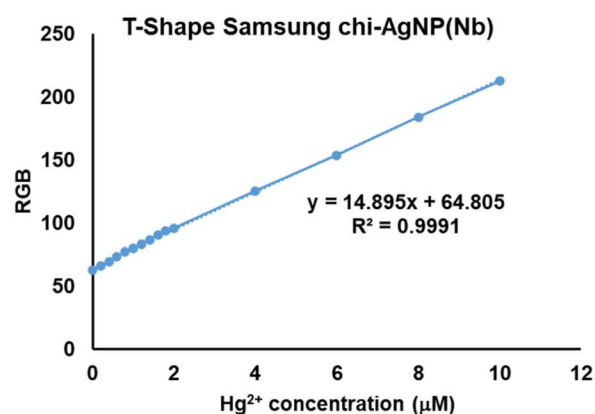
(a)



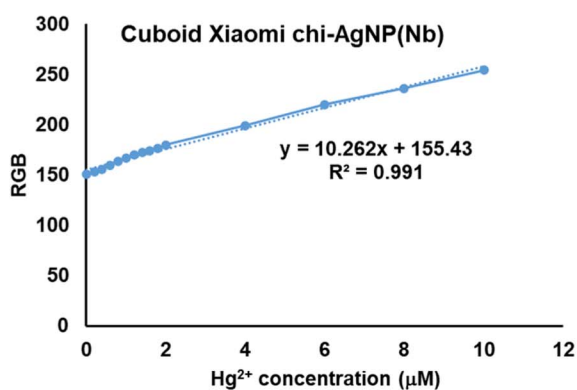
(d)



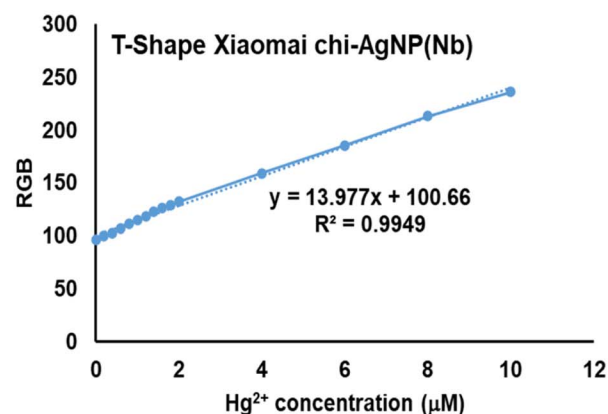
(b)



(e)



(c)



(f)

Fig. 9 The plot of linearity of the average RGB value against various variations in mercury(II) ion concentration; (a–c) data recorded from the cuboid micro-studio; (d–f) data analyzed from the T-shape micro-studio.



Table 2 Detection limit and quantification limit

| Parameters            | UV-vis | Cuboid controlled-light instrument |         |        | T-shape controlled-light instrument |         |        |
|-----------------------|--------|------------------------------------|---------|--------|-------------------------------------|---------|--------|
|                       |        | Asus                               | Samsung | Xiaomi | Asus                                | Samsung | Xiaomi |
| LoD ( $\mu\text{M}$ ) | 0.765  | 0.665                              | 0.621   | 1.324  | 0.573                               | 0.411   | 0.996  |
| LoQ ( $\mu\text{M}$ ) | 2.320  | 2.015                              | 1.882   | 4.014  | 1.737                               | 1.247   | 3.020  |

Table 3 Comparison of the AgNPs paper strip sensitivities on mercury detection

| No. | Silver preparation  | Sensitivity                               | Ref.               |
|-----|---|---|--------------------|
| 1   | Thiamine-functionalized (ThAgNPs), paper strips   | 0.5 $\mu\text{M}$ (naked eye)             | 28                 |
| 2   | Chitosan-Ag $\rightarrow$ chi-AgNP paper strip monitored with smartphone                                | 0.411 $\mu\text{M}$ (LoD for paper strip) | This current study |
| 3   | Sensor: gelatin-functionalized AgNPs paper strips and gel   | 25 nM (undefine LoD)                      | 29                 |
| 4   | AgNPs-methionine test paper and gel   | 20–100 nM (undefine LoD)                  | 30                 |
| 5   | SiO <sub>2</sub> -Ag core-shell NPs-filter paper, PVP-Ag, liquid measurement & computational evaluation | 1.13 nM (undefine LoD)                    | 31                 |

The spectrophotometry method has been popularly used, and its accuracy is convincing, while this chi-AgNP paper strip integrated smartphone has just been introduced. The spectrophotometric method requires a relatively larger volume of chi-AgNPs, which is expensive and requires careful maintenance. The paper strip method uses much less chi-AgNP volume and is portable.

The LoD paper strip reported in this study is comparable to the previous study<sup>28</sup> and less sensitive than other published articles (Table 3). However, the previous reports did not clearly define the paper strip LoD, instead, it seems the sensitivities are reported for the colloidal AgNPs, which is a very different condition from the solid state (paper strip). In addition, the experiment conditions were also different. They used polyvinyl pyrrolidone (PVP), gelatin, methionine, or thiamine as the protecting agents.<sup>28–30</sup> and the AgNPs were core-shell structure with SiO<sub>2</sub> (ref. 31) and not using handphone as the sensor probe for paper strip colour change.

### 3.7 Mercury detection in real water sample using a chi-AgNP(Nb) integrated smartphone

After the chi-AgNP(Nb) paper strip test instruments had been confirmed to detect the very dilute mercury solution (as polluted water simulation) then, the instrument was further tested on various sources of water, including well water, river water (Local River), bottled mineral water (Cleo), and sink water. The chi-

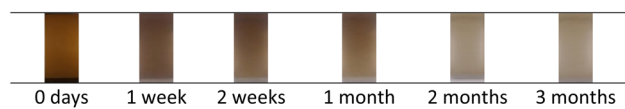


Fig. 11 Colour change of chi-AgNP(Nb) over a certain time period.

AgNP(Nb) paper strip shows no observable colour change, which means the water contains  $<1 \mu\text{M}$  of mercury(II) ions or none. To confirm the instrument sensitivity, the water samples were mixed with  $10 \mu\text{M}$  mercury(II) ions, and then the AgNP(Nb) paper strip turned colourless (Fig. 10). These confirm that the chi-AgNP(Nb) paper strip is applicable in real samples, although the real sample might have many ion interferences.

### 3.8 Expiry period of chi-AgNP(Nb)

During storage, the chi-AgNP(Nb) paper strip changes colour from brown to greyish (Fig. 11), possibly because the colloidal silver nanoparticles gradually change to silver metal, as supported by the previous report.<sup>32</sup> Therefore, to avoid a wrong interpretation of mercury detection, the accuracy of paper strips decreases after a week of storage before use.

## 4. Conclusion

A colorimetric paper strip based on chitosan-silver nanoparticles, chi-AgNP(Nb) confirms the accuracy, including in an actual sample to detect at  $>1 \mu\text{M}$  mercury(II) ions. Almost all metal ions in the sample do not interfere with mercury(II) ion detection. The chi-AgNP(Nb) paper strip assembled with cuboid controlled-light and T-shape controlled-light instruments and integrated with a smartphone and the Color Grab application has no significant difference with UV-vis standard procedure or even better as long as the  $>1 \mu\text{M}$  mercury content within the sample. Therefore, the chi-AgNP(Nb) integrated smartphone is reasonable as a simple, low-cost, and portable instrument for

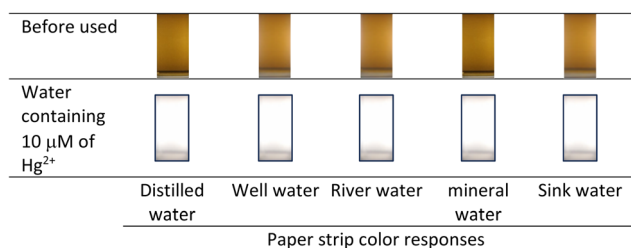


Fig. 10 Colour changes of chi-AgNP(Nb) mixed with various water samples.





the detection of mercury(II) ions within water as long as the mercury pollution is  $>1\ \mu\text{M}$ . Future studies could explore the application of this method in different environmental settings and further improve the sensitivity and selectivity of the paper strips.

## Data availability

All research data have been included in the manuscript; the raw data is available from the corresponding author upon reasonable request. The preliminary research of colloidal chi-AgNPs in liquid state has been published in an IOP conference proceeding: <https://iopscience.iop.org/article/10.1088/1757-899X/352/1/012049>.

## Author contributions

M. Adlim was responsible for designing, guiding the experiment, and drafting the manuscript. M. S. Surbakti and A. F. Omar supervised and developed the conceptual cubic and T-shape micro-studio. R. F. I. Rahmayani performed the experimental data analyses. A. H. Hasmar was involved in assembling and testing the cubic and T-shape micro-studio. I. Ozmen and M. Yavuz confirm contributed by guiding and proofreading the manuscript.

## Conflicts of interest

The authors declare that there is no conflict of interest regarding the publication of this article. The authors confirmed that the paper is free of plagiarism.

## Acknowledgements

We are in debt to Dr Zarlaida Fitri, MSc, who significantly contributed to the laboratory work. She passed away long before the manuscript was written. We thank Universitas Syiah Kuala for the research funding and facilities. Research grant number of 003/UN1.1.D7RKAT-2024-DEV/2023 & ICR-WCU: 1/ UN11.2.1/ PT.01.03/PNBP/2024.

## References

- 1 R. A. Bernhoft, Mercury toxicity and treatment: A review of the literature, *J. Environ. Public Health*, 2012, **2012**, 460508. <https://www.ncbi.nlm.nih.gov/pmc/articles/PMC3253456/>.
- 2 Y. Li, Y. Chen, H. Yu, L. Tian and Z. Wang, Portable and smart devices for monitoring heavy metal ions integrated with nanomaterials, *Trends Anal. Chem.*, 2018, **98**, 190–200. <https://www.sciencedirect.com/science/article/abs/pii/S0165993617303254>.
- 3 F. Zarlaida and M. Adlim, Gold and silver nanoparticles and indicator dyes as active agents in colorimetric spot and strip tests for mercury(II) ions: a review, *Microchim. Acta*, 2017, **184**(1), 45–58. <https://link.springer.com/article/10.1007/s00604-016-1967-4>.
- 4 P. Prema, V. Veeramanikandan, K. Rameshkumar, M. K. Gatasheh, A. A. Hatamleh, B. Ravindran and P. Balaji, Statistical optimization of silver nanoparticle synthesis by green tea extract and its efficacy on colorimetric detection of mercury from industrial wastewater, *Environ. Res.*, 2022, **204**, 111915. <https://www.sciencedirect.com/science/article/abs/pii/S001393512101210X>.
- 5 M. G. Tsegay, H. G. Gebretinsae, J. Sackey, M. Maaza and Z. Y. Nuru, Green synthesis of khat mediated silver nanoparticles for efficient detection of mercury ions, *Mater. Today Proc.*, 2021, **36**, 368–373, Part 2. <https://www.sciencedirect.com/science/article/abs/pii/S2214785320328327>.
- 6 C. Pattnaik, R. Mishra, A. K. Sahu, L. N. Sahoo, N. K. Sahoo, S. K. Tripathy and S. Sahoo, Green synthesis of glucose-capped stable silver nanoparticles: a cost-effective sensor for the selective detection of  $\text{Hg}^{2+}$  ions in aqueous solutions, *Sens. Diagn.*, 2023, **2**(3), 647–656. D3SD00019B. <https://pubs.rsc.org/en/content/articlelanding/2023/sd/d3sd00019b>.
- 7 A. Apilux, W. Siangproh, N. Praphairaksit and O. Chailapakul, Simple and rapid colorimetric detection of  $\text{Hg(II)}$  by a paper-based device using silver nanoplates, *Talanta*, 2012, **97**, 388–394. <https://www.sciencedirect.com/science/article/abs/pii/S0039914012003645>.
- 8 H. E. Kaoutit, P. Estevez, F. C. Garcia, F. Serna and J. M. Garcia, Sub-ppm quantification of  $\text{Hg(II)}$  in aqueous media using both the naked eye and digital information from pictures of a colorimetric sensory polymer membrane taken with the digital camera of a conventional mobile phone, *Anal. Methods*, 2013, **5**, 54–58. C2AY26307F. <https://pubs.rsc.org/en/content/articlelanding/2013/ay/c2ay26307f>.
- 9 L. F. Capitan-vallvey, L. Nuria, A. Martínez-olmos, M. M. Erenas and A. J. Palma, Recent developments in computer vision-based analytical chemistry: A tutorial review, *Anal. Chim. Acta*, 2015, **899**, 23–56. <https://www.sciencedirect.com/science/article/abs/pii/S000326701501243X>.
- 10 S. Kanchi, M. I. Sabela, P. S. Mdluli and K. Bisetty, Smartphone based bioanalytical and diagnosis applications: A review, *Biosens. Bioelectron.*, 2018, **102**, 136–149. <https://www.sciencedirect.com/science/article/abs/pii/S0956566317307509>.
- 11 L.-M. Fu, M.-K. Shih, C.-W. Hsieh, W.-J. Ju, Y.-L. Tain, K.-C. Cheng, J.-H. Hsu, Y.-W. Chen and C.-Y. Hou, Design of an integrated microfluidic paper-based chip and inspection machine for the detection of mercury in food with silver nanoparticles, *Biosensors*, 2021, **11**, 491. bios11120491. <https://pubmed.ncbi.nlm.nih.gov/34940248/>.
- 12 M. M. Bordbar, A. Sheini, P. Hashemi, A. Hajian and H. Bagheri, Disposable Paper-Based Biosensors for the Point of Care Detection of Hazardous Contaminations—A Review, *Biosensors*, 2021, **11**, 316. bios11090316. <https://www.mdpi.com/2079-6374/11/9/316>.
- 13 M. A. T. Safa and H. Koohestani, Green synthesis of silver nanoparticles with green tea extract from silver recycling of



- radiographic films, *Results Eng.*, 2024, **21**, 101808. <https://www.sciencedirect.com/science/article/pii/S2590123024000616>.
- 14 N. George, J. Joy, B. Mathew B and E. P. Koshy, Green mediated synthesis of silver nanoparticle using Euphorbia Maculate leaf extract and their catalytic reduction and antibacterial properties, *Mater. Today Proc.*, 2024, in press. Elsevier <https://www.sciencedirect.com/science/article/abs/pii/S2214785324000130>.
  - 15 E. Z. Okka, T. Tongur, T. T. Aytas, M. Yilmaz, O. Topel and R. Sahin, Green Synthesis and the formation kinetics of silver nanoparticles in aqueous Inula Viscosa extract, *Optik*, 2023, **294**, 171487. <https://www.sciencedirect.com/science/article/abs/pii/S0030402623009853>.
  - 16 A. Rasool, S. Kiran, S. Abrar, S. Iqbal, T. Farooq, N. Jahan, B. Munir, M. Yusuf and N. Mukhtar, Synthesis and characterization of bio-fabricated silver nanoparticles as green catalysts for mitigation of synthetic dyes: A sustainable environmental remedial approach, *J. Mol. Liq.*, 2024, **396**, 124061. <https://www.sciencedirect.com/science/article/abs/pii/S0167732224001168>.
  - 17 Z. Saeed, M. Pervaiz, A. Ejaz, S. Hussain, S. Shaheen, B. Shehzad and U. Younas, Garlic and ginger extracts mediated green synthesis of silver and gold nanoparticles: A review on recent advancements and prospective applications, *Biocatal. Agric. Biotechnol.*, 2023, **53**, 102868. <https://www.sciencedirect.com/science/article/abs/pii/S1878818123002694>.
  - 18 E. A. K. Nivethaa, V. Narayanan and A. Stephen, Synthesis and spectral characterization of silver embedded chitosan matrix nanocomposite for the selective colorimetric sensing of toxic mercury, *Spectrochim. Acta, Part A*, 2015, **143**, 242–250. <https://www.sciencedirect.com/science/article/abs/pii/S1386142515000967>.
  - 19 P. Sharma, M. Mourya, D. Choudhary, M. Goswami, I. Kundu, M. P. Dobhal, C. S. P. Tripathi and D. Guin, Thiol terminated chitosan capped silver nanoparticles for sensitive and selective detection of mercury (II) ions in water, *Sens. Actuators, B*, 2018, **268**, 310–318. <https://www.sciencedirect.com/science/article/abs/pii/S0925400518308268>.
  - 20 A. Adlim, Preparation of Chitosan-Stabilized Silver (Chi-Ag) Nanoparticles Using Different Reducing Agents and Techniques, *J. Sains Teknol.*, 2006, **12**(3), 185–191. <https://jurnal.fmipa.unila.ac.id/index.php/sains/article/view/165>.
  - 21 F. Zarlaida, M. Adlim, M. S. Surbakti and A. F. Omar, Chitosan-stabilized silver nanoparticles for colorimetric assay of mercury (II) ions in aqueous system, *IOP Conf. Ser. Mater. Sci. Eng.*, 2018, **352**, 012049, DOI: [10.1088/1757-899X/352/1/012049](https://doi.org/10.1088/1757-899X/352/1/012049).
  - 22 S. E. F. Kleijn, B. Serrano-Bou, A. I. Yanson and M. T. M. Koper, Influence of Hydrazine-Induced Aggregation on the Electrochemical Detection of Platinum Nanoparticles, *Langmuir*, 2013, **29**(6), 2054–2064, DOI: [10.1021/la3040566](https://doi.org/10.1021/la3040566).
  - 23 J. Alagan and S. Dhesingh, Functionalized silver nanoparticle probe for visual colorimetric sensing of mercury, *Mater. Res. Bull.*, 2016, **83**, 48–55, DOI: [10.1016/j.materresbull.2016.05.029](https://doi.org/10.1016/j.materresbull.2016.05.029).
  - 24 A. Amirjani, F. Firouzi and D. F. Haghshenas, Predicting the Size of Silver Nanoparticles from Their Optical Properties, *Plasmonics*, 2020, **15**, 1077–1082. <https://link.springer.com/article/10.1007/s11468-020-01121-x>.
  - 25 S. K. Vashist and J. H. T. Loung, Smartphone-Based Immunoassays, in *Handbook of Immunoassay Technologies Approaches, Performances, and Applications*, ed. S. K. Vashist and J. H. T. Loung, Academic Press, 2018, ch. 16, pp. 433–453, Copyright © 2018 Elsevier Inc., <https://www.sciencedirect.com/science/article/abs/pii/S0925400518308268>.
  - 26 S. K. Vashist and J. H. T. Loung, Bioanalytical Requirements and Regulatory Guidelines for Immunoassays, in *Handbook of Immunoassay Technologies Approaches, Performances, and Applications*, ed. S. K. Vashist and J. H. T. Loung, Academic Press, 2018, ch. 4, pp. 81–95, Copyright © 2018 Elsevier Inc., <https://www.sciencedirect.com/science/article/abs/pii/S0925400518308268>.
  - 27 Z. Geng, X. Zhang, Z. Fan, X. Lv, Y. Su and H. Chen, Recent progress in optical biosensors based on smartphone platforms, *Sensors*, 2017, **17**(11), 1–19. [s17112449](https://doi.org/10.3390/s17112449). <https://www.mdpi.com/1424-8220/17/11/2449>.
  - 28 M. L. Budlayan, J. Dalagan, J. P. Lagare-Oracion, J. Patricio, S. Arco, F. Latayada, T. Vales, B. Baje, A. Alguno and R. Capangpangan, Detecting mercury ions in water using a low-cost colorimetric sensor derived from immobilized silver nanoparticles on a paper substrate, *Environ. Nanotechnol. Monit. Manage.*, 2022, **18**, 100736, DOI: [10.1016/j.enmm.2022.100736](https://doi.org/10.1016/j.enmm.2022.100736).
  - 29 A. Jeevika and D. R. Shankaran, Functionalized silver nanoparticles probe for visual colorimetric sensing of mercury, *Mater. Res. Bull.*, 2016, **83**, 48–55, DOI: [10.1016/j.materresbull.2016.05.029](https://doi.org/10.1016/j.materresbull.2016.05.029).
  - 30 S. Balasurya, A. Syed, A. M. Thomas, N. Marraiki, A. M. Elgorban, L. L. Raju and S. S. Das, Khan, Rapid colorimetric detection of mercury using silver nanoparticles in the presence of methionine, *Spectrochim. Acta, Part A*, 2020, **228**, 117712, DOI: [10.1016/j.saa.2019.117712](https://doi.org/10.1016/j.saa.2019.117712).
  - 31 A. A. Azmi, A. I. Daud, W. M. Khairul, S. Hamzah, W. M. A. Wan Mohd Khalik and N. H. H. Hairom, Silica-silver core-shell nanoparticles incorporated with cellulose filter paper as an effective colorimetric probe for mercury ion detection in aqueous media: Experimental and computational evaluations, *Environ. Nanotechnol. Monit. Manag.*, 2023, **19**, 100762, DOI: [10.1016/j.enmm.2022.100762](https://doi.org/10.1016/j.enmm.2022.100762).
  - 32 S. Kittler, C. Greulich, J. Diendorf J, M. Köller and M. Eppe, Toxicity of silver nanoparticles increases during storage because of slow dissolution under release of silver ions, *Chem. Mater.*, 2010, **22**(16), 4548–4554. [cm100023p](https://pubs.acs.org/doi/10.1021/cm100023p). <https://pubs.acs.org/doi/10.1021/cm100023p>.

